Biosensors and Bioelectronics 180 (2021) 113100

Contents lists available at ScienceDirect

Biosensors and Bioelectronics

journal homepage: http://www.elsevier.com/locate/bios

Ultra-sensitive surface enhanced Raman spectroscopy sensor for in-situ monitoring of dopamine release using zipper-like ortho-nanodimers

Lang Li, Yang Lu, Ziting Qian, Zhaoyan Yang, Kuo Yang, Shenfei Zong, Zhuyuan Wang *, Yiping Cui

Advanced Photonics Center, School of Electronic Science and Engineering, Southeast University, Nanjing, 210096, Jiangsu, China

ARTICLE INFO

Keywords:
SERS
Sensor
Dopamine
3D culture
Microfluidic chip

ABSTRACT

Accurate quantitative detection of dopamine (DA) in blood is essential for the early diagnosis and the pathogenesis analysis of dopaminergic dysfunction, which still remains a great challenge because of the extremely low concentration in patients. Using our previously reported DNA-assisted synthesis of ortho-nanodimers (DaSON) strategy, a microfluidic surface enhanced Raman spectroscopy (SERS) biosensor for the ultrasensitive and reliable detection of DA in serum was demonstrated by modifying SERS probes with DA aptamers in a specific orientation to form zipper-like ortho-nanodimers. The uniform 1-nm gap in zipper-like ortho-nanodimers endows the SERS sensor with ultrahigh sensitivity and high accuracy for the detection of DA. The limit of detection is as low as 10 aM in phosphate buffer saline and 10 fM in serum, which is about two orders of magnitude lower than that of previous methods. Using a single microfluidic chip containing a 3D cell culture unit, quantitatively in-situ monitoring of extracellular DA released from living neurons under different medications was first realized. Quantification of DA in human blood samples was also achieved with the recoveries ranging from 87.5% to 123.7%. Given the difficulty of DA quantification in complex physiological samples, our developed SERS sensor provides an appealing tool for in-vitro investigating of neurological processes and clinical examination of dopaminergic disorders.

1. Introduction

Neurotransmitters are a series of messenger molecules that transmit information in human body and maintain the balance of physiological function, which play important roles in emotion regulation and behaviors, learning and cognitive activities, homeostasis, individual movements control and coordination (Blokland, 1995; Dulcis et al., 2013; Tse et al., 1976; van den Pol, 2003). Dysregulation of neurotransmitters is strongly associated with diseases such as mental disease, cognitive disorders and angiocardiopathy (Kurian et al., 2011; Sawa and Snyder, 2002; Stagg et al., 2011; Wulff et al., 2010).

Dopamine (DA) is one of the most common neurotransmitters which regulates physiological processes in nervous, hormonal and cardiovascular systems (Clarke and Guttman, 2002; Goerendt et al., 2003; Liss and Roeper, 2008). Deficiency of DA causes clinical symptoms such as Parkinson's disease, depression and schizophrenia (Hoglinger et al., 2004; Sawa and Snyder, 2002; Xu et al., 2002). In clinical practice, DA level is a key index for the diagnosis and therapy of dopaminergic dysfunction. Quantification of DA is not only critical for clinical blood examination of these dopaminergic dysfunctions, but also important for the *in-vitro* investigating of DA-related neuronal signaling pathway and neurological processes. However, the rapid detection of DA in clinical samples remains a great challenge due to the low basal level and the complex physiological environment (Davis et al., 1991; Sharma et al., 2019). Although various methods have been proposed for the determination of DA in physiological samples, there are intrinsic drawbacks for these approaches. For example, electrochemical method is restricted by the specificity and stability due to the strong interference from other biomolecules (e.g. ascorbic acid and uric acid) (Huang et al., 2008; Li et al., 2013). Chromatographic method requires expensive instruments and time-consuming operation (Cannazza et al., 2005). Colorimetric methods are difficult to achieve a high sensitivity (Yin et al., 2019; Zhu et al., 2019). Hence, in order to meet the stringent requirements of DA detection in real physiological samples, a novel method with high sensitivity, high selectivity and high accuracy is strongly demanded by clinical medicine.

* Corresponding author.
E-mail address: wangzy@seu.edu.cn (Z. Wang).

https://doi.org/10.1016/j.bios.2021.113100
Received 16 January 2021; Received in revised form 14 February 2021; Accepted 15 February 2021
Available online 18 February 2021

Surface enhanced Raman spectroscopy (SERS) is regarded as an effective sensing technique due to its superiority in high sensitivity, non-invasive, rich spectral information and multiplexing capability. Over the last decades of exploration and development, SERS technique has been extensively applied for biosensing including proteins (Cheng et al., 2017; Wang et al., 2017), nucleic acids (Xu et al., 2015a) and exosomes (Dong et al., 2020). Unfortunately, direct SERS detection of DA in blood is difficult due to the low concentration, the small Raman cross section of DA, as well as the complex interference from sample matrix (Viet-Duc et al., 2018; Wang et al., 2015). Hence, a variety of SERS probes with specific targeting capability and strong SERS signal for DA detection have been developed (Zhang et al., 2018). Overview these probes, DNA aptamer has usually been considered as an ideal targeting ligand owing to its flexibility, programmability and specificity, while nanoparticle assemblies such as dimers are used to generate strong SERS signals due to the strong electromagnetic enhancement in the gap between nanoparticles (An et al., 2015; Tang et al., 2015). However, the gap in conventional DNA-based dimers is too wide to provide strong enough signals due to the formation of rigid double-strand DNA (Xu et al., 2015b). Besides, the uniformity is also defective considering the inhomogeneous SERS enhancement factor and the biological background signal (Fang et al., 2019). Thus, high sensitivity and high uniformity are still two major barriers of SERS technique towards practical applications. Recently, we have reported a strategy named as DNA-assisted synthesis of ortho-nanodimers (DaSON) which is able to produce precisely-controlled sub-nanoscale interparticle gap between Ag nanoparticles and generate great plasmonic enhancement with excellent reproducibility of SERS signals (Li et al., 2020).

Herein, inspired by the DaSON strategy, a highly sensitive SERS sensor with salient signal uniformity was presented by forming zipper-like nanodimers with uniform 1-nm interparticle gap, which suits well for the quantitative detection of biomolecules in complex body fluid such as blood. Fig. 1a shows the fabrication of DaSON strategy-based SERS sensor. First, Ag substrate was fabricated by the electrostatic self-assembly of Ag nanoparticles on the glass slide. The thiolated complementary DNAs of DA aptamer were modified onto the surfaces of Ag nanoparticles through Ag–S bond. Then, SERS probes were synthesized by decorating Ag nanoparticles with DA aptamers and Raman reporter as 5,5′-Dithiobis-(2-nitrobenzoic acid) (DTNB). Afterwards, the obtained SERS probes were added to bind with the complementary DNA on the substrate. By simply inversing the orientation of DA aptamers on the SERS probes, zipper-like ortho-nanodimers with 1-nm gap can be formed between the SERS probes and the Ag nanoparticles on the substrate under the equilibrium state of electrostatic repulsion and the hybridization contractility. Finally, DA-contained samples were added for detection, the stronger affinity between DA and DA aptamer can release the SERS probes from the substrate, resulting in DA concentration-dependent weakening of SERS intensity of DTNB. Compared to the conventional DNA-assisted Ag dimer, the huge electromagnetic field enhancement inside 1-nm gap can increase SERS intensity for more than one order of magnitude and improve the signal uniformity to less than 5%, resulting in the ultrahigh sensitivity and accuracy for the detection of DA. By introducing the SERS sensor and a three-dimensional (3D) cell culture unit into a single microfluidic chip, quantitatively in-situ monitoring of DA release from living neurons was directly realized without any sample pretreatment, and the different response of DA release under various medication can be observed, indicating of foreseeable application prospects for in-vitro neurological investigation and drug efficacy evaluation. Besides, the SERS sensor is also able to achieve a rapid and accurate quantitative determination of DA in real blood samples, showing its great potential in clinical practice.

2. Materials and methods

2.1. Reagents and instruments

Poly dimethyl diallyl ammonium chloride (PDDA), and 5,5′-Dithiobis-(2-nitrobenzoic acid) (DTNB) were purchased from Sigma Aldrich.

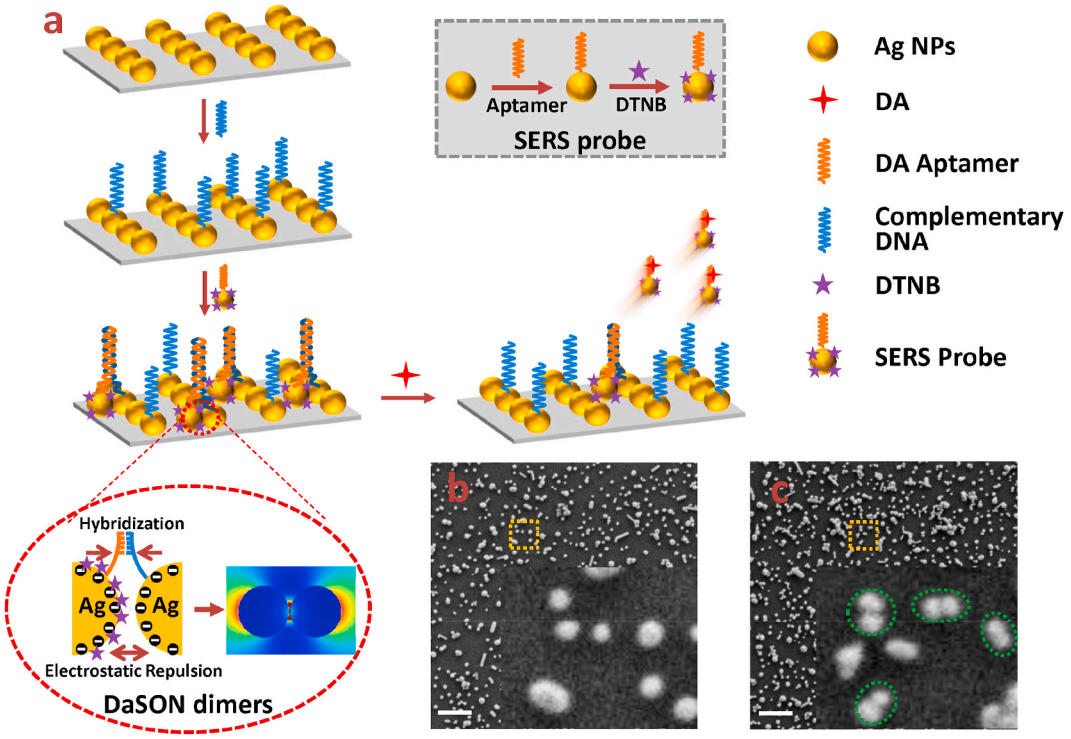

Fig. 1. Configuration of the SERS sensor. (a) The schematic illustration of the DaSON strategy-based SERS sensor for the detection of DA. The SEM images of the SERS sensor (d) before and (e) after the adsorption of SERS probes, the insets are the enlarged view of the yellow rectangle, the scale bar is 500 nm. (For interpretation of the references to colour in this figure legend, the reader is referred to the Web version of this article.)

Silver nitrate ($AgNO_3$), gold acid chloride trihydrate ($HAuCl_4{\cdot}4H_2O$) and dopamine (DA) were purchased from Alfa-Aesar. DNAs were purchased from Shanghai Sangon Biotech Co., Ltd. Sodium citrate was purchased from Sinopharm Chemical Reagent Co., Ltd. Phosphate buffered saline (PBS, 10 mM, PH = 7.4) was purchased from Wuhan Boster Biological Technology., Ltd. All solvents and reagents were of analytical grade and used without further purification. Glass slides were purchased from Haimen Xinxing experiment company. PDMS microfluidic chips were purchased from Suzhou Wenhao chip technology Co., Ltd.

DA aptamer: 5′-GTCTCTGTGTGCGCCAGAGAACACTGGGGCAG ATATGGGCCAGCACAGAATGAGGCCC–SH–3'.

Complementary DNA: 5-SH-GGGCCTCATTCTGTGCTGGCCCATATC TGCCCCAGTGTTCTCTGGCGCACACAGAGAC.

SERS spectra was measured with a Raman spectroscopy (T64000, Horiba, Japan). TEM images were obtained by a transmission electron microscope (FEI Tecnai G2T20). SEM figures were obtained by a scanning electron microscope (Zeiss Ultra Plus). UV−Vis spectra were recorded by a UV-Vis spectrometer (UV-3600, Shimazu, Japan). Injection pump (LSP04-1A) was purchased from Longer Precision Pump Co., Ltd.

2.2. Synthesis of Ag nanospheres (Lee and Meisel, 1982)

44 mg of $AgNO_3$ was dissolved in 245 mL of deionized water in an erlenmeyer flask, the mixed solution was heated to boiling under stirring conditions. 50 mg of sodium citrate dissolved in deionized water was added into the erlenmeyer flask to react for 45 min and then naturally cooled. Ag nanospheres were ready for use after centrifugation (4163 rcf, 15 min).

2.3. Synthesis of Au and Au@Ag nanospheres

100 μL of $HAuCl_4{\cdot}4H_2O$ was added into 100 mL of deionized water in an erlenmeyer flask, the mixed solution was heated to boiling under stirring condition. 40 mg of sodium citrate dissolved in 4 mL deionized water was added into the erlenmeyer flask to react for 45 min and then naturally cooled. Au nanospheres were ready for use after centrifugation (5437 rcf, 20 min). To synthesize Au@Ag nanospheres, 20 mg of $AgNO_3$ and 40 mg of sodium citrate dissolved in 4 mL deionized water were added to the obtained solution of Au nanospheres.

2.4. Preparation and hybridization of DNA-modified nanoprobes (Zhang et al., 2012)

1 mL of Ag NPs solution was centrifuged and re-suspended in 1 mL of deionized water, then 20 μL of thiolated DNA and 30 μL of citrate-HCl buffer (pH = 3) were added orderly under stirring. After 30 min, 10 μL of DTNB (10 mM) was added to bind with Ag NPs for 20 min. Then, 10 μL of salmon sperm DNA was added and kept stirring for another 30 min to reduce the nonspecific adsorption. Finally, the obtained solution was centrifuged and re-suspended in PBS. The process was the same for Au nanoparticles or Au@Ag core-shell nanoparticles.

In order to obtain zipper-like ortho-nanostructures, two kinds of nanoprobes that modified with complementary DNAs were equal-proportionally mixed and incubated in 37 °C for 12 h.

2.5. Fabrication of SERS substrates in microfluidic chips

First, the PDMS chips were sonicated in EtOH for 30 min with microfluidic channels (width:500 μm, height:100 μm) on their surfaces. Then, the microfluidic chips were prepared by bonding the PDMS chips with the glass slides, which have been previously sonicated with piranha solution. The SERS substrates used in the microfluidic chip were prepared by electrostatic interaction between the negatively charged Ag nanospheres and positive charged PDDA. Briefly, in the first step, 30 μL of 1 wt. % PDDA solution was injected (0.5 μL/min) into the microfluidic chips, followed by 3-min of water washing at a flow rate of 2 μL/min. PDDA molecules were adsorbed on the glass slide due to the presence of hydroxy groups. Second, the solution of Ag nanospheres was injected (0.5 μL/min) into the microfluidic chip to interact with PDDA through electrostatic force, followed by 3-min of deionized water washing at a flow rate of 2 μL/min. Then, a layer of Ag nanospheres was successfully assembled on the microfluidic channel as a SERS substrate.

2.6. SERS sensing of DA

The as-prepared SERS substrate in microfluidic chip was modified with thiolated complementary DNA of DA aptamer, and sealed by salmon sperm DNA. Then, the aptamer-modified SERS probe was injected to hybridize with its complementary DNA and form zipper-like ortho-nanostructure. Afterwards, DA-contained samples (30 μL) were injected to bind with the aptamer, resulting in the desorption of SERS probes and the decrease of SERS signal.

After reaction, SERS signal was measured using a confocal Raman spectroscopy. The laser wavelength was 633 nm and the laser power was 2 mW. The integration time was set as 5 s. The obtained SERS intensity was used to calculate the concentration of DA in sample, the standard deviation of SERS intensity was calculated as the error bar.

2.7. 3D culture of PC12 cells in the microfluidic chip

The 3D culture unit of microfluidic chip contains one central channel (width: 1 mm, length: 1 cm) for cell culture and two side channels (width: 1.5 mm, length: 1 cm) for the addition of culture medium. The side channels and the central channel were separated by a row of discrete hexagonal columns (side length: 400 μm) allowing the culture medium to flow through. The gap between hexagonal columns is 200 μm. For 3D cell culture, 100 μL of deionized water, 65 μL of 100 mM PBS, 50 μL of 0.1 M NaOH and 280 μL of collagen were mixed, followed by the addition of 500 μL of PC12 cell suspension. The cell-contained pre-hydrogel was added into the cell culture channel and left standing at 37 °C for 30 min. Then, 1640 cell culture medium (containing 10% FBS) was added to the side channel. The 3D-culture microfluidic chip was incubated at 37 °C before SERS sensing. To determine the released concentration of DA, 30 μL of the culture medium from the 3D culture unit was pumped into the detection unit. SERS signal was measured after reaction. The obtained SERS intensity was used to calculate the concentration of DA in sample.

2.8. Drug-stimulated DA release

To study the effect of medication on the DA release from PC12 cells, the cell culture in microfluidic chip was replaced with fresh cell culture containing different concentration of L-dopa or K^+, and followed by incubation for a certain time. Then the culture medium was pumped into the sensing area for DA detection.

2.9. DA determination in blood samples

Human blood samples in this experiment were obtained from Zhongda Hospital, affiliated to the Southeast University, China. Our study received ethics approval and no-informed consent from the ethics committee of Zhongda Hospital, affiliated to the Southeast University (2018ZDSYLL024-P01). The blood samples were centrifuged to obtain serum, then the serum was collected and diluted (10%) for SERS determination without further process. For DA recovery in blood, DA at different concentration was added into the blood samples. The mixture was then processed into serum for SERS detection. To determine the concentration of DA in serum, 30 μL of the diluted serum was injected to react with the SERS sensor. SERS signal was measured after reaction.

3. Results and discussion

3.1. Characterization of the SERS sensor

Ag nanoparticles (Ag NPs) with an average size of 40 nm were synthesized through the sodium citrate reduction methods, which exhibits a SPR peak at 404 nm (Supplementary Fig. S1). (Lee and Meisel, 1982) Then, Ag nanoprobes were prepared by sequentially decorating the Ag NPs with 5′-thiolated DA aptamer and the Raman reporter as DTNB (5, 5′-Dithiobis-(2-nitrobenzoic acid), using an acid assisted method (Zhang et al., 2012). A new P2p peak can be observed in the XPS spectrum of Ag nanoprobes, indicating the successful decoration of DNA (Supplementary Fig. S1-d). The zeta potential shows a negative surface charge of both Ag NPs and Ag nanoprobes (Supplementary Fig. S2).

Fig. 1a shows the schematic diagram for the SERS sensing of DA. Specifically, the 3′-thiolated complementary DNAs of DA aptamer are modified on the self-assembled monolayer Ag NPs substrate through Ag–S bond (Fig. 1b). Then, the aptamer-decorated SERS probes are added to allow for the hybridization of DNA, which results in the formation of the zipper-like ortho-nanodimers (Fig. 1c). DA-contained samples are subsequently added to specifically bind with the aptamer, leading to the detachment of SERS probes from the substrate. Thus, SERS intensity weakens in a concentration-dependent manner of DA. In conventional DNA-based dimers (Supplementary Fig. S3), Ag nanoparticles located in the opposite side of the double-strand DNA, the gap width usually varies from several to a dozen nanometers (depends on the length of DNA) because of the stiffness of double-strand DNA, which limits the enhancement of SERS signal (Acuna et al., 2012). However, as we have previously demonstrated (Li et al., 2020), in our DaSON strategy, two Ag nanoparticles are located at the same end of the double-strand DNA. The two Ag nanoparticles get closer and closer under the hybridization of DNA, until the gap width is narrow enough so that the electrostatic repulsion force of nanoparticles can neutralize the contractility force of DNA. The final gap width is determined by the equilibrium state of hybridization contractility and the electrostatic repulsion, thus the gap width can be tuned from sub-nanometer to several nanometers by changing the surface charge of nanoparticles (e.g. pH environment) or the parameters of DNA chains (e.g. length or mismatch). As the surface charge of nanoparticles and the hybridization contractility are constant for certain DNA and the environment, the gap in dimer is extremely narrow (~1 nm) and uniform. It has been reported that the narrow gap can provide much stronger enhancement factor (EF) (Li et al., 2019a, 2019b; Ma et al., 2017). Hence, such a uniform 1-nm gap contributes to both the dramatically enhanced SERS intensity (with an EF of 2.33×10^{10}) and the excellent signal uniformity. As shown in Fig. 2a and b, the signal intensity of our SERS sensor is about 1 order of magnitude stronger than that from conventional Ag dimer, and the relative standard deviation (RSD) of SERS signal from different points is only 4.16%, which is much lower than that of conventional strategy (~11.5%).

3.2. Optimization of the SERS sensor

In order to optimize the performance of the SERS sensor, we evaluated the effect of nanoparticles and DNA on SERS signals. First, Au nanoparticles (Au NPs) and Au@Ag core-shell nanoparticles (Au@Ag NPs) instead of Ag nanoparticles were used to fabricate the SERS sensor (Supplementary Fig. S4). Although SERS intensity of DaSON-based SERS sensor enhanced for all three kinds of nanoparticles with a magnification factor about 10 when compared to the conventional strategy-based sensor, the signal intensity using Ag NPs was much stronger than that by Au NPs or Au@Ag NPs (Fig. 2b and Supplementary Fig. S5). Hence, Ag NPs were used in the following sensing experiments.

On the other hand, the parameters of DNA also affect the

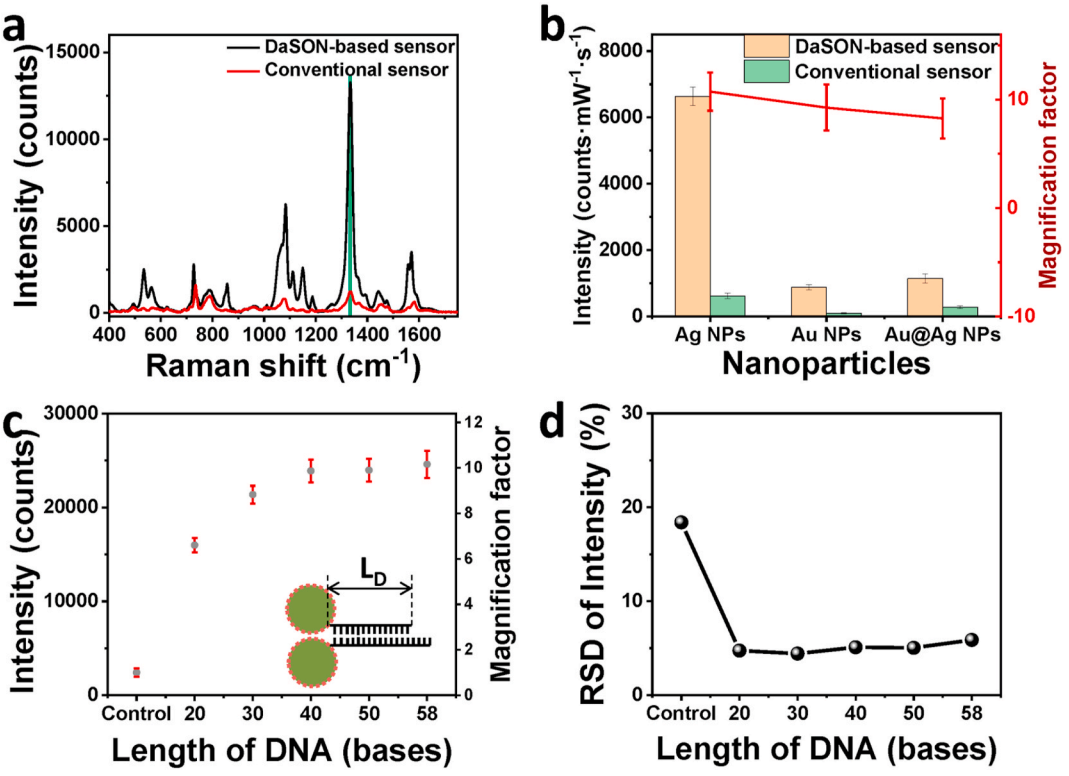

Fig. 2. SERS performance of the SERS sensor based on DaSON strategy. (a) SERS intensity obtained from the DaSON strategy-based SERS sensor and from the conventional strategy. (b) Comparison of SERS intensity from both DaSON-based SERS sensor and conventional dimer-based SERS sensor using three different kinds of nanoparticles. The influence of the length of complementary DNA on (c) SERS intensity and (d) SERS uniformity. SERS signals from conventional strategy are used as the control.

performance of such a SERS sensor. In our experiments, the length of the complementary DNA and the mismatch in DNA were adjusted to evaluate their influences on the sensor. As shown in Fig. 2c and d, in the beginning, the SERS intensity enhanced with the increasing length of complementary DNA, and then remained stable for DNA length beyond 40 bases. Such an evolution is possibly caused by the difficulty for shorter DNA to get close and hybridize under the electrostatic repulsion between two Ag nanoparticles. Importantly, for all the DNA length covering from 20 to 58 bases, the RSD of SERS signal kept as low as around 5%, which can meet with the requirement for quantitative detection. Moreover, the mismatch of DNA sequence closed to Ag nanoparticles reduced both the signal intensity and homogeneity of the SERS sensor (Supplementary Fig. S6). This could be attributed to the weakening of the hybridization contractility and the generation of flexible single-strand DNA, which results in the wider gap width in dimers. Therefore, in the following experiments of DA sensing, the completely complementary DNA to DA aptamer was used to fabricate the SERS sensor.

3.3. Quantitative DA detection

For the detection of DA, the SERS substrate was first modified with complementary DNA of DA aptamer, then DA aptamer-modified Ag nanoprobes were added to form zipper-like nanodimers which provide strong SERS signals. With the presence of DA, the aptamer-modified SERS probe will be released from the substrate due to the stronger binding force between DA and its aptamer, which leads to the broken of zipper-like nanodimers as well as the decrease of SERS intensity. Since a higher concentration of DA results in weaker SERS signals, the correlation between DA concentration and SERS intensity can be used for quantitative detection of DA. Fig. 3a shows the variation of SERS signal after the addition of DA solution (in PBS) at different concentration. It shows that the SERS intensity is negatively correlated to the concentration of DA. A calibration curve can be established utilizing the correlation between SERS intensity and the concentration of DA (Fig. 3b). As shown in the figure, the sensor exhibits an ultra-high sensitivity for the detection of DA, the limit of detection (LOD) is as low as 10 aM, much lower than those previously reported methods (Rasheed and Lee, 2017; Tang et al., 2015; Tukimin et al., 2018; Yusoff et al., 2015). Besides, the linear detection range is from 1 fM to 10 pM with a R-squared of 0.9979, indicating of a wide dynamic sensing range with a good linearity. Meanwhile, the SERS sensor holds an excellent uniformity (<5%) for the whole linear detection range. For example, for DA at 10 fM, according to the SERS spectra obtained from ten random positions, the relative standard deviation of the intensity at 1333 cm^{-1} is as low as 3.94% (Fig. 3c and Supplementary Fig. S7). Such an ultra-high sensitivity and excellent uniformity of the SERS sensor declares its great potential for the reliable quantification of DA in the practical applications.

3.4. In-situ monitoring of DA release under drug stimulation

Detection of DA in practical application usually accompanies with the complex environments. In order to validate the feasibility of our SERS sensor in the complex body fluids, DA in the serum environments was detected and the results are shown in Fig. 4a. It shows that the SERS sensor retains its high sensitivity for DA even in the serum environment, owing to the high affinity of aptamer to DA and the strong SERS

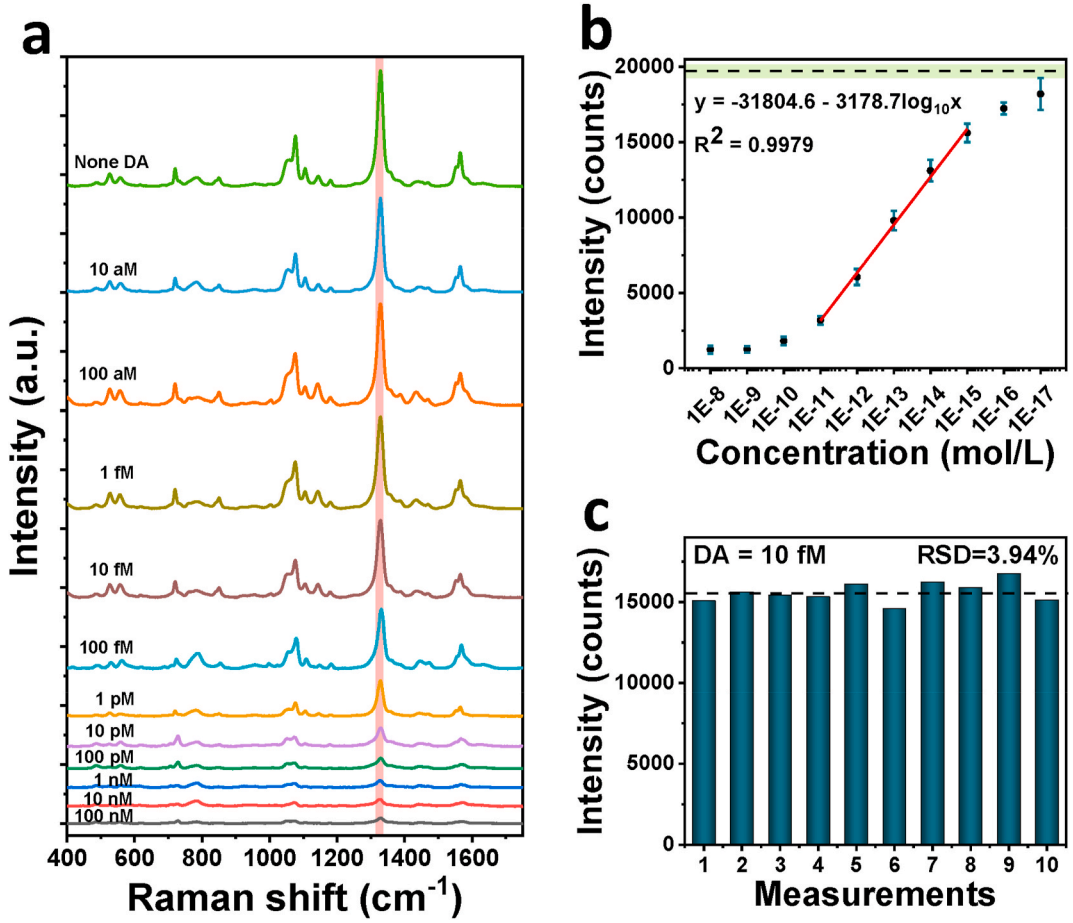

Fig. 3. SERS sensing results of DA. (a) SERS spectra for sensing DA at different concentration; (b) Calibration curve between SERS intensity at 1333 cm^{-1} and the concentration of DA; (c) Uniformity for the detection result of DA (10 fM).

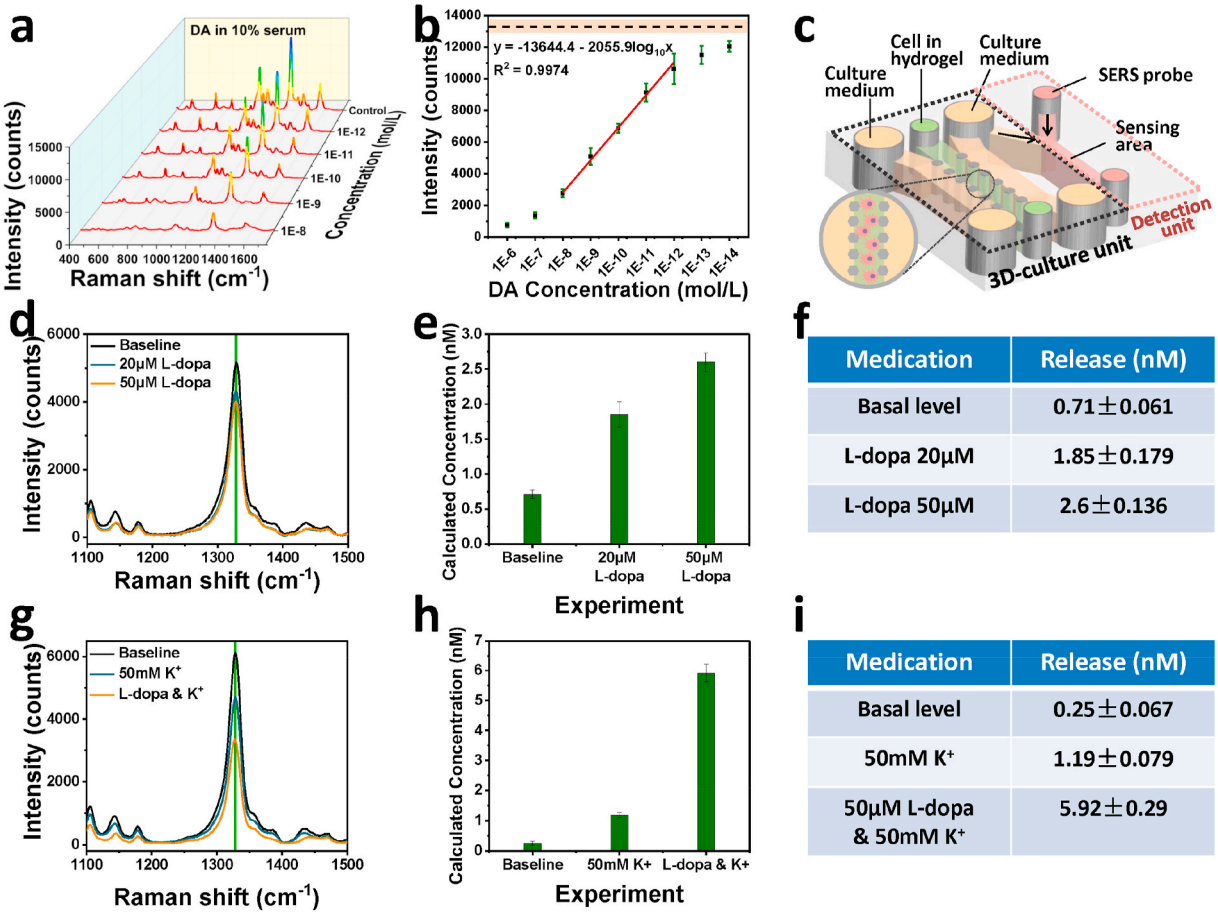

Medication	Release (nM)
Basal level	0.71±0.061
L-dopa 20μM	1.85±0.179
L-dopa 50μM	2.6±0.136

Medication	Release (nM)
Basal level	0.25±0.067
50mM K^+	1.19±0.079
50μM L-dopa & 50mM K^+	5.92±0.29

Fig. 4. Monitoring results of DA released from living PC12 cells. (a, b) Calibration curve re-established in serum environment. (c) Schematic illustration of the microfluidic chip for in-situ monitoring of DA release from living PC12 cells. (d–f) Effect of L-dopa on the release of DA from PC12 cells. (g–i) The co-stimulation of K^+ and L-dopa on DA release from PC12 cells.

enhancement. The re-established calibration curve (Fig. 4b) shows a linear detection range from 1 pM to 10 nM with a LOD of 10 fM, the shift of the calibration curve towards higher concentration is mainly ascribed to the interference of complex serum compositions. The background interference results in the decrease of the sensitivity as well as the shift of the calibration curve. As far as we know, this is the most sensitive DA sensor under serum environment with such a wide dynamic range (Alvarez-Martos et al., 2019; Azadbakht et al., 2016; Liu et al., 2012; Sun et al., 2018; Wang et al., 2015). Moreover, the uniformity of the detection was also well remained in serum environment. As shown in Supplementary Fig. s8, for DA at 100 pM, the RSD is as low as 4.15%, which can meet the requirement for the quantitative determination. As previously reported (Olefirowicz and Ewing, 1990), the extracellular concentration of DA of neurons is about 10^{-10} M. The clinical level of DA in undiluted human serum or blood plasma is between 1 nM (a basal level) (Hashizume et al., 1995) and 0.9–6 μM (in L-dopa-treated parkinson's patients) (Riggin et al., 1976). Hence, the sensitivity of our SERS sensor is fully competent for the determination of DA in different physiological samples. The specificity of the sensor towards DA against other molecules and ions in serum was also tested (Supplementary Fig. S9), which shows a good selectivity of SERS response towards DA. The detection reliability of the sensor was evaluated by comparing with an ELISA kit, the results (Supplementary Fig. S10) show good consistence between two methods.

In-situ monitoring of DA release from living neurons can facilitate the *in-vitro* drug screening and provide a unique insight for DA-related neuronal signaling pathway and neurological processes, which has been difficult to realize due to the limitation of the detection sensitivity and the difficulty of in-situ observation. The 3D culture techniques in microfluidic chips have attracted an increasing attention because of its vivid mimicking of in-vivo stereoscopic environment and high operability. Hence, by introducing the SERS sensor into a 3D culture microfluidic chip, in-situ monitoring of DA release from living neurons can be facilely achieved. Rat adrenal pheochromocytoma (PC12) cell, a kind of highly differentiated sympathetic-like neurons, was used as the neuron model (Li et al., 2013; Westerink and Ewing, 2008). A schematic illustration of the microfluidic chip for monitoring in-situ release of DA from living PC12 cells is shown in Fig. 4c, which contains a cell culture unit and a detection unit. In the 3D-culture unit, PC12 cells were cultured in the central hydrogel network and surrounded by culture medium in side channel. The typical shape of PC12 cells could be observed in the 3D-culture unit (Supplementary Fig. S11). In the detection unit, the DaSON-based SERS sensor was fabricated on the substrate of the microfluidic channel. After incubating PC12 cells for a certain time under various medication, the culture medium consisting of the released DA was pumped from the 3D culture unit into the detection unit for in-situ monitoring of DA release.

Levodopa (L-dopa) is a clinically-used pro-drug for the treatment of Parkinson's disease, which can be transformed to DA in neurons to increase the level of DA (Cotzias et al., 1969; Pothos et al., 1996). Using the 3D microfluidic-SERS system, we investigated the effect of L-dopa on the DA release from the living neurons. As shown in Fig. 4d and f, the basal level for the release of DA was about 0.71 ± 0.061 nM after 1 h of culture. The addition of 20 μM of L-dopa into the culture medium increased the extracellular level of DA to 1.85 ± 0.179 nM while 50 μM of L-dopa can further increase the level of DA to 2.6 ± 0.136 nM, which

is about 2.6 and 3.7 times higher than basal level respectively. Such a concentration-dependent increase of DA release is well consistent with clinical effects (Everett and Borcherding, 1970).

It is well known that high concentration of potassium ion (K^+) can promote the release of DA from neurons (Greene and Rein, 1977; Kumar et al., 1998; Li et al., 2013). To further prove the capability of the DaSON-based SERS sensor for in-situ monitoring of DA release, PC12 cells were incubated in culture medium that containing 50 mM K^+ for 15 min and the concentration of DA in culture medium was then detected. As shown in Fig. 4g–i, the basal level of DA release without the stimulation of K^+ was about 0.25 ± 0.067 nM. After 15 min of incubation in 50 mM K^+, the DA release increased to 1.19 ± 0.079 nM, the release amount of DA was increased by about 4.76 times under the stimulation of 50 mM K^+. Surprisingly, the co-incubation of K^+ and L-dopa with PC12 cells shows much stronger stimulation effect. The PC12 cells were pretreated with 50 μM L-dopa for 1 h, followed by an incubation of 50 mM K^+ for 15 min. Then, the released DA was detected to be 5.92 ± 0.29 nM, which is about 23.68 times higher than the basal level. The release amount of DA under the combination of L-dopa and K^+ was much larger than that under either single stimulation. Considering the different roles of L-dopa and K^+ in the release of DA (Kumar et al., 1998; Pothos et al., 1996), it can be deduced that the pretreatment of L-dopa promotes the synthesis of DA in neurons and leads to the increased storage of DA in neurons. Thus, DA can be released rapidly under the stimulation of K^+, resulting in the significantly increased amount of DA release under co-stimulation. These results provide a new insight into DA releasing response of neurons under external drug stimulation, which also demonstrate the potential of this microfluidic-SERS system for *in-vitro* drug screening.

3.5. Quantitative DA determination in blood sample

Quantitative determination of DA in blood sample is of great significance for the clinical diagnosis and the accurate medication of related diseases (Iversen and Iversen, 2007; Schultz, 2007). Here, our SERS sensor was applied for blood test to validate its feasibility in point-of-care application.

The temporal stability of the sensor was first tested, which shows a good stability in 4 days and slightly degeneration after one week (Supplementary Fig. S12). Whole blood samples from healthy person were processed into serum by centrifugation and then diluted to 10%. Then, the concentration of DA in 10% serum was detected using the SERS sensor and calculated according to the calibration curve in Fig. 4b. As shown in Fig. 5, the basal level of DA in the diluted human serum sample 1(H1) and human serum sample 2 (H2) was 0.14 ± 0.042 nM and 0.056 ± 0.027 nM, respectively, which is consistent with the clinical level of

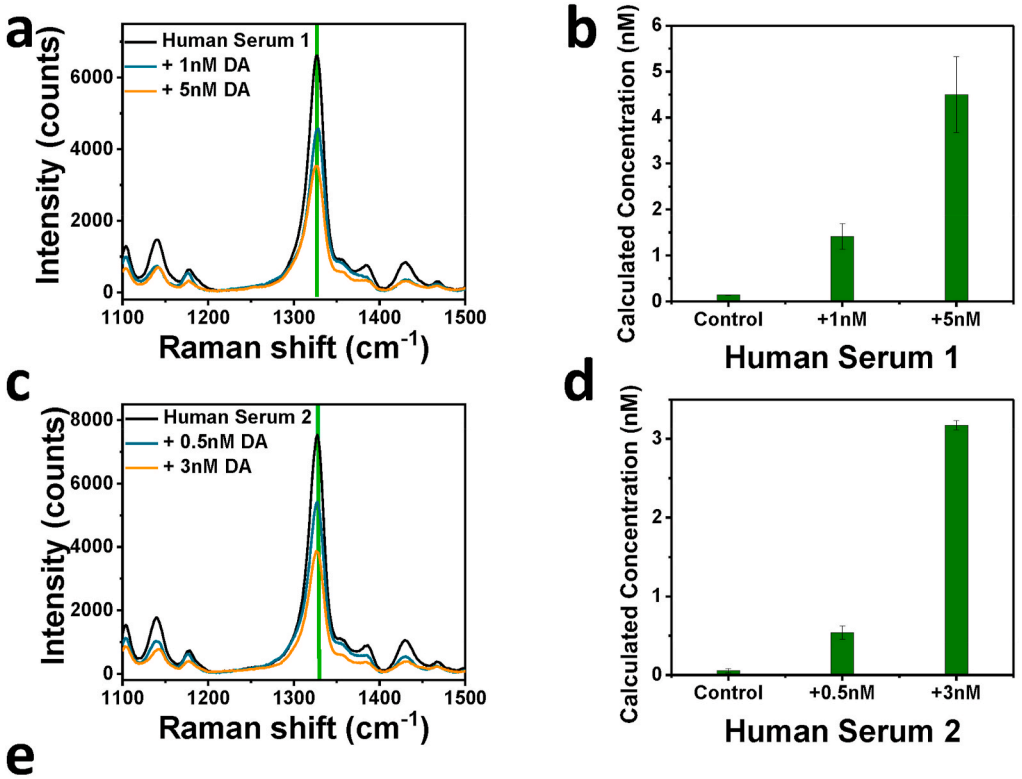

e

Blood Sample (10%)	Added (nM)	Found (nM)	Recovery (%)
H1 (0.14nM)	1	1.41±0.28	123.7
H1 (0.14nM)	5	4.5±0.83	87.5
H2 (0.056nM)	0.5	0.54±0.085	97
H2 (0.056nM)	3	3.17±0.61	103.7

Fig. 5. SERS sensing of DA in human blood samples. (a, b) SERS spectra and the calculated concentration of DA in 10% human serum 1; (c, d) SERS spectra and the calculated concentration of DA in 10% human serum 2; (e) The concentration of DA after its addition to blood sample in 10% human serum sample.

healthy individuals (Hashizume et al., 1995).

Afterwards, for more evidences to prove the detecting ability of our SERS sensor, the increase of DA in blood was measured after the addition of DA into the blood samples. The detection results are shown in Fig. 5a–d. Obviously, the SERS intensity decreased with the addition of DA into blood samples, the calculated concentrations of DA are compared with the actual final concentration (Fig. 5e). The results show good recoveries ranging from 87.5% to 123.7%, indicating of the good accuracy and great potential of the SERS sensor for the clinical applications.

4. Conclusion

In summary, a highly sensitive SERS sensor with uniform signals was facilely achieved through the formation of DaSON-based zipper-like ortho-nanodimers. Compared with the conventional DNA-based SERS sensor, the sensing strategy using DaSON can enhance the signal intensity by more than 1 orders of magnitude while remain an excellent signal uniformity. Thus, such a SERS sensor helps to resolve two major limitations – sensitivity and uniformity – in the way of practical SERS application. The multiple-parameter analysis demonstrates that this SERS sensor can also be fabricated using other metal nanoparticles as Au or Ag NPs. Besides, DNA sequences can be designed to adjust the SERS performance. For example, longer DNAs with completely complementary base pairs exhibit stronger SERS intensity due to a greater chance of hybridization.

When the SERS sensor was used for the detection of DA, both an ultra-high sensitivity (LOD = 10 aM) and a super-excellent uniformity (RSD<5%) were achieved. Meanwhile, even under the complex serum environment, the SERS sensor remains good feasibility and stability in a linear dynamic range covering from 1 pM to 10 nM, suiting well for the concentration level of DA in most physiological samples such as blood or cerebrospinal fluid. Using such a SERS sensor, quantitative determination of dopamine in human blood samples can be successfully achieved with good recoveries, providing a powerful tool for the clinical diagnosis of DA-related diseases. In addition, by combining with microfluidic technique, 3D neuron model was established and then integrated with the SERS sensor into single chip. In-situ monitoring of DA that released from living PC12 neurons under different medication was directly performed without any sample pretreatment, the results demonstrate that the co-incubation of K^+ and L-dopa with PC12 neurons shows synergistic stimulated effect on DA release. Therefore, such a SERS sensor with ultra-high sensitivity and excellent uniformity not only shows a great potential for the clinical examination of DA level, but also holds a broad prospect in the future *in-vitro* investigation of neurological processes, pharmacodynamic assessment or drug screening.

CRediT authorship contribution statement

Lang Li: Conceptualization, Methodology, Writing – original draft. **Yang Lu:** Formal analysis, Investigation, Visualization. **Ziting Qian:** Resources. **Zhaoyan Yang:** Resources. **Kuo Yang:** Validation. **Shenfei Zong:** Writing – review & editing. **Zhuyuan Wang:** Writing – review & editing, Funding acquisition. **Yiping Cui:** Funding acquisition.

Declaration of competing interest

The authors declare that they have no known competing financial interests or personal relationships that could have appeared to influence the work reported in this paper.

Acknowledgement

This study was supported by the State Key Program of National Natural Science Foundation of China (Grant No. 61535003), the National Science Fund for Excellent Young Scholars (Grant No. 61822503) and the National Natural Science Foundation of China (Grant No. 61675042).

Appendix A. Supplementary data

Supplementary data to this article can be found online at https://doi.org/10.1016/j.bios.2021.113100.

References

Acuna, G.P., Moeller, F.M., Holzmeister, P., Beater, S., Lalkens, B., Tinnefeld, P., 2012. Science 338 (6106), 506–510.
Alvarez-Martos, I., Moller, A., Ferapontova, E.E., 2019. ACS Chem. Neurosci. 10 (3), 1706–1715.
An, J.H., Choi, D.-K., Lee, K.-J., Choi, J.-W., 2015. Biosens. Bioelectron. 67, 739–746.
Azadbakht, A., Roushani, M., Abbasi, A.R., Menati, S., Derikvand, Z., 2016. Mater. Sci. Eng. C-Mater. Biol. Appl. 68, 585–593.
Blokland, A., 1995. Brain Res. Rev. 21 (3), 285–300.
Cannazza, G., Di Stefano, A., Mosciatti, B., Braghiroli, D., Baraldi, M., Pinnen, F., Sozio, P., Benatti, C., Parenti, C., 2005. J. Pharmaceut. Biomed. Anal. 36 (5), 1079–1084.
Cheng, Z., Choi, N., Wang, R., Lee, S., Moon, K.C., Yoon, S.-Y., Chen, L., Choo, J., 2017. ACS Nano 11 (5), 4926–4933.
Clarke, C.E., Guttman, M., 2002. Lancet 360 (9347), 1767–1769.
Cotzias, G.C., Ps, Papavasi, Gellene, R., 1969. N. Engl. J. Med. 280 (7), 337.
Davis, K.L., Kahn, R.S., Ko, G., Davidson, M., 1991. Am. J. Psychiatr. 148 (11), 1474–1486.
Dong, S., Wang, Y., Liu, Z., Zhang, W., Yi, K., Zhang, X., Zhang, X., Jiang, C., Yang, S., Wang, F., Xiao, X., 2020. ACS Appl. Mater. Interfaces 12 (4), 5136–5146.
Dulcis, D., Jamshidi, P., Leutgeb, S., Spitzer, N.C., 2013. Science 340 (6131), 449–453.
Everett, G.M., Borcherding, J.W., 1970. Science 168 (3933), 849–+.
Fang, Q., Li, Y., Miao, X., Zhang, Y., Yan, J., Yu, T., Liu, J., 2019. Analyst 144 (11), 3649–3658.
Goerendt, I.K., Messa, C., Lawrence, A.D., Grasby, P.M., Piccini, P., Brooks, D.J., 2003. Brain 126, 312–325.
Greene, L.A., Rein, G., 1977. Brain Res. 129 (2), 247–263.
Hashizume, K., Yamatodani, A., Ogihara, T., 1995. Hypertens. Res. Off. J. Jpn. Soc. Hypertens. 18 (Suppl. 1), S205–S207.
Hoglinger, G.U., Rizk, P., Muriel, M.P., Duyckaerts, C., Oertel, W.H., Caille, I., Hirsch, E. C., 2004. Nat. Neurosci. 7 (7), 726–735.
Huang, J., Liu, Y., Hou, H., You, T., 2008. Biosens. Bioelectron. 24 (4), 632–637.
Iversen, S.D., Iversen, L.L., 2007. Trends Neurosci. 30 (5), 188–193.
Kumar, G.K., Overholt, J.L., Bright, G.R., Hui, K.Y., Lu, H.W., Gratzl, M., Prabhakar, N.R., 1998. Am. J. Physiol. Cell Physiol. 274 (6), C1592–C1600.
Kurian, M.A., Gissen, P., Smith, M., Heales, S.J.R., Clayton, P.T., 2011. Lancet Neurol. 10 (8), 721–733.
Lee, P.C., Meisel, D., 1982. J. Phys. Chem. 86 (17), 3391–3395.
Li, B.-R., Hsieh, Y.-J., Chen, Y.-X., Chung, Y.-T., Pan, C.-Y., Chen, Y.-T., 2013. J. Am. Chem. Soc. 135 (43), 16034–16037.
Li, J., Heng, H., Lv, J., Jiang, T., Wang, Z., Dai, Z., 2019a. Small 15 (48).
Li, J., Koo, K.M., Wang, Y., Trau, M., 2019b. Small 15 (50).
Li, L., Wang, Z., Lu, Y., Zhu, K., Zong, S., Cui, Y., 2020. Biosens. Bioelectron. 172, 112769-112769.
Liss, B., Roeper, J., 2008. Brain Res. Rev. 58 (2), 314–321.
Liu, S., Xing, X., Yu, J., Lian, W., Li, J., Cui, M., Huang, J., 2012. Biosens. Bioelectron. 36 (1), 186–191.
Ma, W., Fu, P., Sun, M., Xu, L., Kuang, H., Xu, C., 2017. J. Am. Chem. Soc. 139 (34), 11752–11759.
Olefirowicz, T.M., Ewing, A.G., 1990. J. Neurosci. Methods 34 (1–3), 11–15.
Pothos, E., Desmond, M., Sulzer, D., 1996. J. Neurochem. 66 (2), 629–636.
Rasheed, P.A., Lee, J.-S., 2017. Microchimica Acta 184 (5), 1239–1266.
Riggin, R.M., Alcorn, R.L., Kissinger, P.T., 1976. Clin. Chem. 22 (6), 782–784.
Sawa, A., Snyder, S.H., 2002. Science 296 (5568), 692–695.
Schultz, W., 2007. Annu. Rev. Neurosci. 30, 259–288.
Sharma, N.S., Acharya, S.K., Nair, A.P., Matalia, J., Shetty, R., Ghosh, A., Sethu, S., 2019. Indian J. Ophthalmol. 67 (1), 38–41.
Stagg, C.J., Bachtiar, V., Johansen-Berg, H., 2011. Curr. Biol. 21 (6), 480–484.
Sun, F., Zeng, J., Jing, M., Zhou, J., Feng, J., Owen, S.F., Luo, Y., Li, F., Wang, H., Yamaguchi, T., Yong, Z., Gao, Y., Peng, W., Wang, L., Zhang, S., Du, J., Lin, D., Xu, M., Kreitzer, A.C., Cui, G., Li, Y., 2018. Cell 174 (2), 481–+.
Tang, L., Li, S., Han, F., Liu, L., Xu, L., Ma, W., Kuang, H., Li, A., Wang, L., Xu, C., 2015. Biosens. Bioelectron. 71, 7–12.
Tse, D.C.S., McCreery, R.L., Adams, R.N., 1976. J. Med. Chem. 19 (1), 37–40.
Tukimin, N., Abdullah, J., Sulaiman, Y., 2018. J. Electrochem. Soc. 165 (7), B258–B267.
van den Pol, A.N., 2003. Neuron 40 (6), 1059–1061.
Viet-Duc, P., Jung, W.-S., Thuy-An, N., Kim, J.-H., Lee, S.-W., 2018. Nanoscale 10 (47), 22493–22503.
Wang, P., Xia, M., Liang, O., Sun, K., Cipriano, A.F., Schroeder, T., Liu, H., Xie, Y.-H., 2015. Anal. Chem. 87 (20), 10255–10261.
Wang, Z., Zong, S., Wu, L., Zhu, D., Cui, Y., 2017. Chem. Rev. 117 (12), 7910–7963.
Westerink, R.H.S., Ewing, A.G., 2008. Acta Physiol. 192 (2), 273–285.
Wulff, K., Gatti, S., Wettstein, J.G., Foster, R.G., 2010. Nat. Rev. Neurosci. 11 (8), 589–+.

Xu, J., Kao, S.Y., Lee, F.J.S., Song, W.H., Jin, L.W., Yankner, B.A., 2002. Nat. Med. 8 (6), 600–606.
Xu, L.-J., Lei, Z.-C., Li, J., Zong, C., Yang, C.J., Ren, B., 2015a. J. Am. Chem. Soc. 137 (15), 5149–5154.
Xu, L., Yan, W., Ma, W., Kuang, H., Wu, X., Liu, L., Zhao, Y., Wang, L., Xu, C., 2015b. Adv. Mater. 27 (10), 1706–+.
Yin, M., Li, S., Wan, Y., Feng, L., Zhao, X., Zhang, S., Liu, S., Cao, P., Wang, H., 2019. Chem. Commun. 55 (80), 12008–12011.
Yusoff, N., Pandikumar, A., Ramaraj, R., Lim, H.N., Huang, N.M., 2015. Microchimica Acta 182 (13–14), 2091–2114.
Zhang, K., Liu, Y., Wang, Y., Zhang, R., Liu, J., Wei, J., Qian, H., Qian, K., Chen, R., Liu, B., 2018. ACS Appl. Mater. Interfaces 10 (18), 15388–15394.
Zhang, X., Servos, M.R., Liu, J., 2012. J. Am. Chem. Soc. 134 (17), 7266–7269.
Zhu, J., Peng, X., Nie, W., Wang, Y., Gao, J., Wen, W., Selvaraj, J.N., Zhang, X., Wang, S., 2019. Biosens. Bioelectron. 141.